Influence of skull flexibility during closed head impact

Ronald van den Akker

February 4, 2010

Department of Applied Mechanics
Division of Fluid Dynamics
Division of Vehicle Safety
Chalmers University of Technology
Göteborg Sweden, 2009.

Abstract

Numerical simulations are of big interest for the research of closed head impact brain injuries. Especially to understand the mechanisms in the head during the impact and on the other hand to improve the existing numerical models and to advance the material theories. This report is about the development of the a human head model which include solids parts as well as a fluid part. It focuses on the mechanisms of the human head.

In addition, several theories explained why the brain injury is placed frontal part (coup injury) or in the opposite site of the impact (contrecoup injury) during an impact at the front side of the head. Also the influence of the density of the cerebrospinal fluid (CSF) is still a major point of discussion. Besides the discussion about the density of the CSF also skull flexibility is of big interest, but it is not investigated in research so far.

For the simulation of the skull and brain surrounding the CSF, the computational fluid dynamics software Ansys CFX was coupled with the finite element software Ansys Workbench. A major part of the project was to generate a good working mesh and to chose the right configuration for the fluid part of the model. Also the implementation of the coupled simulation was very time consuming.

Unfortunately there was a calculation error discovered in the earlier work of this study, just before the end of the project. The results obtained are therefore not reliable enough.

Despite there were a lot of problems at the end of the project, it is still believed that the skull flexibility has an influence on brain injuries during a closed head impact. Still there is a lot work to do in this research to improve vehicle safety and to improve the understanding of brain injuries during a closed head impact.

Acknowledgment

I want to thank my two supervisors from the department of Applied Mechanics. Special thanks to Professor Lars Davidson, of the Division of Fluid Mechanics, and Professor Mats Svensson, from the Division of Vehicle Safety, for the great support and encouragement during the research. Also the stimulating discussions were very helpfull and instructive.

I would like to thank Dorien van de Belt with helping to find this internship. Without her help this internship would never have become accomplished.

Generally, thanks to all the people at the department for their help and discussions during the nice coffee breaks.

Finally I would like to thank Peyman Jafarian, Martina Blom and Ilyas Yilmaz for being such a nice colleagues during my period in Göteborg.

Nomenclature

Abbreviations

CFD	Computational fluid dynamics
CSF	Cerebrospinal fluid
DAI	Diffuse axonal injury
EDH	Epidural hematoma
FE	Finite element
FEM	Finite element method
FVM	Finite volume method
PDE	Partial differential equations
TBI	Traumatic Brain Injury

Symbols

α	Thermal expansion coefficient
β	Bulk modulus
κ	Isothermal compressibility term
λ	Conductivity
μ	Viscosity
μ^v	Volume viscosity coefficient
ν	Poisson ratio
ρ	Density
τ	Stress tensor
$\mathbf{\Psi}$	Constitutive equation
$\mathbf{\Psi_{def}}$	Deformation part of the constitutive equation
c	Speed of sound

d	Incompressibility term
h	Enthalpy
m	Mass
p	Pressure
t	Time
u	Displacement vector
$\dot{u}$	Velocity vector
$\ddot{u}$	Acceleration vector
C	Damping matrix
E	Young's modulus
J	Jacobi determinant
K	Stiffness matrix
M	Mass matrix
R	Load vector
$\mathbf{S_E}$	Source term
$\mathbf{S_M}$	Source term
T	Temperature
∇T	Temperature gradient
V	Volume

Contents

List of Figures

Preface

This report describes how a numerical model of the human head can be made. In chapter 1 a brief motivation is given, which can be found in section 1.1. In section 1.2 the anatomy of the human head (skull, CSF and brain) is described. Then several brain injuries are discussed in section 1.3. A literature review about prescribing different model of head injuries is given in section 1.4. Finally the scope of the project can be found in section 1.5.

Chapter 2 describes the methodology of the different computer software which are used in this study. The finite element method program ANSYS WORKBENCH is described in section 2.1. Then the computational fluid dynamics (CFD) program ANSYS CFX is discussed in section 2.2. The coupling between this two programs can be found in section 2.3.

The proposed model of this research is described in chapter 3. First the pre-processing is discussed in section 3.1, which includes the geometry and mesh. The description of the solution route is given in section 3.2.

In chapter 4 the results are analysed. First the model of Sans and Aracil is discussed in section 4.1 and then the results of section 4.2 are discussed.

Finally some conclusions and recommendations are given in chapter 5.

1 Introduction

1.1 Motivation

Around the globe traumatic brain injury (TBI) is the leading cause of death and disability. It is the number one cause of coma, it plays the leading role in disability due to trauma, and is the leading cause of brain damage in children and young adults [1]. In Europe it is responsible for more years of disability than any other cause. It also plays a significant role in half of trauma deaths.

Findings on the frequency of each level of severity vary based on the definitions and methods used in studies. A World Health Organization study estimated that between 70 and 90% of head injuries that receive treatment are mild. The incidence of TBI varies by age, gender, region and other factors. The annual incidence of mild TBI is difficult to determine but may be 100–600 people per 100000 [2].

The incidence of TBI is increasing globally, largely due to an increase in motor vehicle use in low- and middle-income countries. In developing countries, automobile use has increased faster than safety infrastructure could be introduced. In contrast, vehicle safety laws have decreased rates of TBI in high-income countries, which have seen decreases in traffic-related TBI since the 1970s. In the European Union the yearly aggregate incidence of TBI hospitalizations and fatalities is estimated at 235 per 100000 [1].

The most common causes of TBI include violence, transportation accidents, construction, and sports. In the US, falls account for 28% of TBI, motor vehicle accidents for 20%, being struck by an object for 19%, violence for 11%, and non-motor vehicle bicycle accidents for 3% [3]. Bicycles and motor bikes are major causes, with the latter increasing in frequency in developing countries. The estimates that between 1.6 and 3.8 million traumatic brain injuries each year are a result of sports and recreation activities in the US. In children aged two to four, falls are the most common cause of TBI, while in older children bicycle and auto accidents compete with falls for this position.

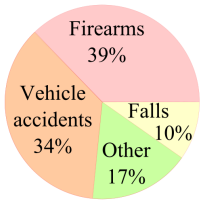

Figure 1.1: Causes of TBI fatalities in the US. [4]

To understand how the brain gets injured during an accident, the mechanical response

of the contents of the head during impact has to be known. Since this mechanics in the human head cannot be determined during an experiment, numerical finite element (FE) modeling is often used to predict the mechanics. Current FE head models contain a detailed geometrical description of anatomical components inside the head but lack accurate descriptions of the brain material behavior and contact between skull and brain. Also, the numeric solution method used in current models does not provide accurate predictions of transient phenomena in the nearly incompressible brain material and the cerebrospinal fluid (CSF).

The aim of this study is to contribute to the improvement of FE head models used to predict the mechanics in the human head during a closed head impact. Because of the continuing development of computer technologies it is possible to run impact simulations on personal computers instead of supercomputers. The topics of research are the influence flexibility of the skull and the density of the CSF during a closed head impact on the mechanics in the human head.

1.2 The anatomy of the human head

To ease the understanding of the mechanics during a closed head impact the different parts of the human head will be discussed. The model in this study will contain the skull, the CSF and the brain, so only these three components will be discussed in the following three sections.

1.2.1 Human skull

The adult skull is normally made up of 22 bones. Except for the mandible, all of the bones of the skull are joined together by sutures, immovable joints formed by bony ossification, with perforating fibers permitting some flexibility [4].

Eight bones form the neurocranium (brain case), a protective vault of bone surrounding the brain and brain stem. Fourteen bones form the splanchnocranium, which comprises the bones supporting the face. Encased within the temporal bones are the six auditory ossicles of the middle ear. The hyoid bone, supporting the larynx, is usually not considered as part of the skull, as it is the only bone that does not articulate with other bones of the skull.

The skull also contains the sinus cavities, which are air-filled cavities lined with respiratory epithelium, which also lines the large airways. The exact functions of the sinuses are debatable; they contribute to lessening the weight of the skull with a minimal reduction in strength, they contribute to resonance of the voice, and assist in the warming and moistening of air drawn in through the nasal cavities. The bone of the skull is build in three layers; the external table, the diploe and the internal table. The diploe is a spongy kind of bone between the two tables, see figure 1.2b.

In history a lot of research is done on the mechanical properties of the human skull [5, 6, 7]. From this literature the mechanical properties, like density and the Young's modulus, can be determined. In section 3.1 these properties are shown.

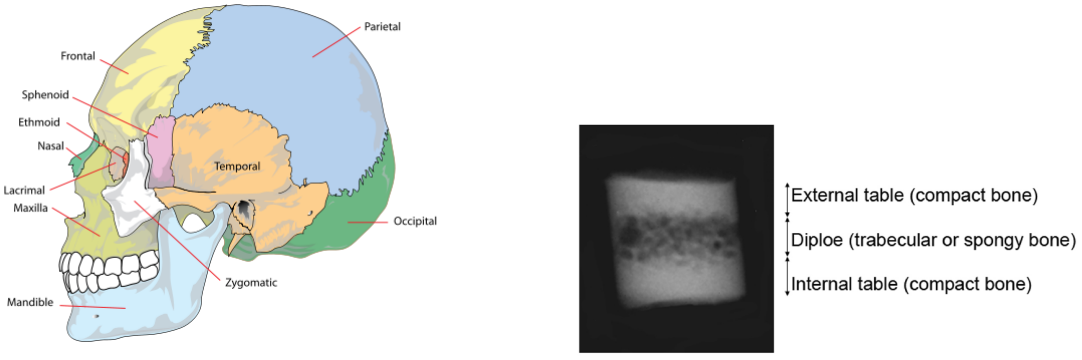

a b

Figure 1.2: Different parts of the human skull (a) and the three layers [5] (b)

1.2.2 Cerebrospinal fluid

CSF is a clear bodily fluid that occupies the subarachnoid space and the ventricular system around and inside the brain. In essence, the brain "floats" in it. The CSF occupies the space between the arachnoid mater (the middle layer of the brain cover, meninges), and the pia mater (the layer of the meninges closest to the brain). The CSF constitutes the content of all intra-cerebral (inside the brain, cerebrum) ventricles, cisterns, and sulci (singular sulcus), as well as the central canal of the spinal cord. It acts as a "cushion" or buffer for the cortex, providing a basic mechanical and immunological protection to the brain inside the skull. It is produced in the choroid plexus.

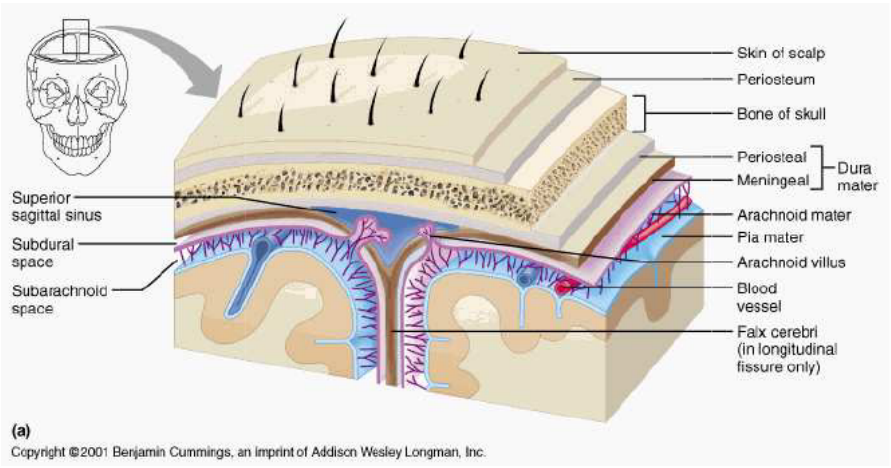

Figure 1.3: Meningeal layers. [10]

The CSF is produced at a rate of 500 $^{ml}/_{day}$. Since the brain can contain only from 135 to 150 ml, large amounts are drained primarily into the blood through arachnoid

granulations in the superior sagittal sinus. Thus the CSF turns over about 3.7 times a day. This continuous flow into the venous system dilutes the concentration of larger, lipoinsoluble molecules penetrating the brain and CSF [8]. The CSF contains approximately 0.3% plasma proteins, or 15 to 40 $^{mg}/_{dL}$, depending on sampling site. CSF pressure is around $< 200\ mmH_20$ (1.94 kPa) in normal children and adults, with most variations due to coughing or internal compression of jugular veins in the neck [9].

In literature the density of the CSF is still a matter of debate [11, 12]. Some believe that the density of the CSF is less than the brain, where others believe the opposite. Because of this discussion the density of the CSF will be a variable during the simulations.

1.2.3 Human brain

The human brain is the center of the human nervous system and is a highly complex organ. The anatomy of the brain is complex due to its intricate structure and function. This organ acts as a control center by receiving, interpreting, and directing sensory information throughout the body. There are three major divisions of the brain. They are the forebrain, the midbrain, and the hindbrain [13].

The forebrain is responsible for a variety of functions including receiving and processing sensory information, thinking, perceiving, producing and understanding language, and controlling motor function. There are two major divisions of forebrain: the diencephalon and the telencephalon. The diencephalon contains structures such as the thalamus and hypothalamus which are responsible for such functions as motor control, relaying sensory information, and controlling autonomic functions. The telencephalon contains the largest part of the brain, the cerebral cortex. Most of the actual information processing in the brain takes place in the cerebral cortex [13].

The midbrain and the hindbrain together make up the brainstem. The midbrain is the portion of the brainstem that connects the hindbrain and the forebrain. This region of the brain is involved in auditory and visual responses as well as motor function [13].

The hindbrain extends from the spinal cord and is composed of the metencephalon and myelencephalon. The metencephalon contains structures such as the pons and cerebellum. These regions assists in maintaining balance and equilibrium, movement coordination, and the conduction of sensory information. The myelencephalon is composed of the medulla oblongata which is responsible for controlling such autonomic functions as breathing, heart rate, and digestion [13].

The adult human brain weighs on average about 1.5 kg with a size of around 1130 cm^3 in women and 1260 cm^3 in men [14, 16], although there is substantial individual variation. Men's brains are on average 100 g heavier than a woman's, even when corrected for body size differences [15].

For the mechanical properties of the brain Francheschini [17] did an interesting research on this subject. In section 3.1 these properties are given.

1.3 Head injuries

Head injuries include both injuries to the brain and those to other parts of the head, such as the scalp and skull. Head injuries may be closed or open. A closed head injury is one in which the skull is not broken. A penetrating head injury occurs when an object pierces the skull and breaches the dura mater. Brain injuries may be diffuse, occurring over a wide area, or focal, located in a small, specific area.

Concussion

Mild concussions are associated with sequelae. However, a slightly greater injury is associated with both anterograde and retrograde amnesia (inability to remember events before or after the injury). The amount of time that the amnesia is present correlates with the severity of the injury. In all cases the patients develop postconcussion syndrome, which includes memory problems, dizziness, tiredness, sickness and depression. Cerebral concussion is the most common head injury seen in children [19].

Epidural hematoma

Epidural hematoma (EDH) is a rapidly accumulating hematoma between the dura mater and the cranium. These patients have a history of head trauma with loss of consciousness, then a lucid period, followed by loss of consciousness. Clinical onset occurs over minutes to hours. Many of these injuries are associated with lacerations of the middle meningeal artery. A "lenticular", or convex, lens-shaped extracerebral hemorrhage will likely be visible on a CT scan of the head. Although death is a potential complication, the prognosis is good when this injury is recognized and treated [20].

Subdural hematoma

Subdural hematoma occurs when there is tearing of the bridging vein between the cerebral cortex and a draining venous sinus. At times they may be caused by arterial lacerations on the brain surface. Acute subdural hematomas are usually associated with cerebral cortex injury as well and hence the prognosis is not as good as extra dural hematomas. Clinical features depend on the site of injury and severity of injury. Patients may have a history of loss of consciousness but they recover and do not relapse. Clinical onset occurs over hours. A crescent shaped hemorrhage compressing the brain will be noted on CT of the head. Craniotomy and surgical evacuation are required if there is significant pressure effect on the brain.Complications include focal neurologic deficits depending on the site of hematoma and brain injury, increased intra cranial pressure leading to herniation of brain and ischemia due to reduced blood supply and seizures [18].

Cerebral contusion

Cerebral contusion is bruising of the brain tissue. The majority of contusions occur in the frontal and temporal lobes. Complications may include cerebral edema and transtentorial herniation [18].

Diffuse axonal injury

Diffuse axonal injury (DAI) usually occurs as the result of an acceleration or deceleration motion, not necessarily an impact. Axons are stretched and damaged when parts of the brain of differing density slide over one another. Prognoses vary widely depending on the extent of damage [21].

1.4 Literature review

In this section some articles will be reviewed. Until now a lot research is done on FE models of the human head. Because it is a very interesting topic, this review will discuss some articles that have done research into FE modeling for head injuries. Also have to be noticed that the statements and opinions made in these articles are made by the authors themselves.

1.4.1 Development and validation of a new finite element model of human head. [22]

In 2005 Belingardi *et al.* made an finite element model of the human head. The brain tissue is modeled as a visco-elastic material and the skull as linear elastic. Despite the CSF is a fluid it is modeled as a linear elastic material. The geometrical model of the head has been built by taking advantage of CT scan and MRI images. More than 160 CT scan images corresponding to sections at a 1.25 mm distances of a 31 year old patient with a cranium trauma without serious cerebral consequences have been used to build the internal and external surfaces of the cranium and the facial bones.

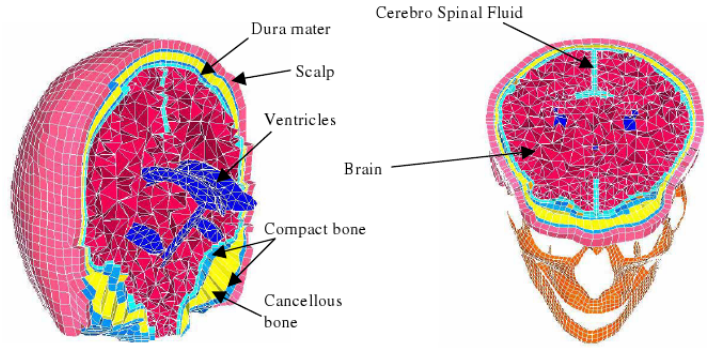

Figure 1.4: Coronal and axial section of the head model. [22]

Results and conclusions

Figure 1.5 shows the pressure distribution on a median sagittal section. A gradual transition from compression in the frontal zone to tension in the occipital zone can be observed. This is due to inertia forces that push the brain against the frontal portion of the skull and pull it from the occipital portion leading to large stresses in the connecting tissues between brain and bone. After the first bounce the brain return in the equilibrium position (about $t = 6.3\,ms$). The pressure distribution comes back to normality but the relative velocity between brain and skull, due to different inertial properties, creates the countercoup effect when the brain is compressed towards the occipital zone (about $t = 7.3\,ms$). The analysis of the pressure distribution in different moments allows also to study the load transfer mechanism from the impacted area of the skull to the brain. In particular it is worth to notice the time delay of the mechanical responses in bone tissues and in the brain: high pressure values are reached in the bone about $1.8\,ms$ after impact while brain is still floating in the CSF and maximum values of pressure are reached after about $4.4\,ms$ in brain.

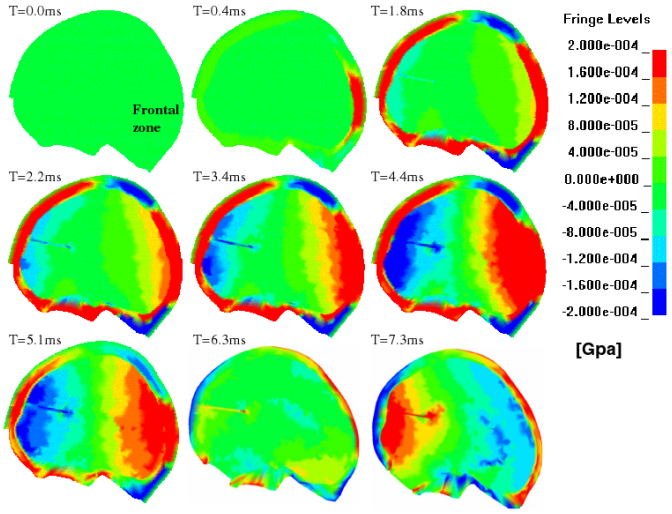

Figure 1.5: Pressure distribution on a sagittal section during impact. [22]

1.4.2 Simulation mechanism of brain injury during closed head impact. [26]

This paper studied the mechanics of the brain during closed head impact via numerical simulation. It proposed a mathematical model of the human head, which consists of three layers: the rigid skull, the cerebrospinal fluid and the solid brain, see figure 1.6. During the simulations the CSF density is fixed at 1000 kg/m^3, and the brain density varies from 500 kg/m^3 to 1500 kg/m^3. The fluid behavior is governed by the Navier-Stokes equations, and the fluid and solid interact together according to the laws of mechanics. Numerical simulations are then performed on this model to simulate accident scenarios. Several theories have been proposed to explain whether the ensuing brain injury is dominantly located at the site of impact (coup injury) or at the site opposite to it (contrecoup

injury). In particular, it investigated the positive pressure theory, the negative pressure theory, and the cerebrospinal fluid theory. It assumes that CSF is denser than brain tissue. Thus, the brain at impact is propelled to the contrecoup location due to the CSF moving forward towards the coup site. The simulation is in two phases. In the first phase the head is accelerating horizontally and in the second phase the head is at impact, thus decelerating and velocity are zero. Contrecoup injuries are usually dominant and coup injuries are minor or absent for this kind of simulations.

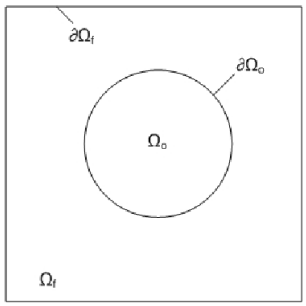

Figure 1.6: The proposed head model with the three layers: skull ($\partial\Omega_f$), CSF (Ω_f), and the brain (Ω_o)

Results and conclusions

In the first phase of the simulation, if brain tissue is denser than CSF, as the head accelerates forward, the brain lags behind. On the other hand, if CSF is denser, then the brain also moves forward. Larger density difference results in larger velocity of the brain; however, the direction of motion is unchanged.

In the second phase, if the brain is denser, as the head comes to a stop, the brain continues to more forward inside the head. On the other hand, if CSF is denser, then the brain moves backward.

As mentioned, there are three main theories that have been developed to explain the coup-contrecoup phenomenon. The positive pressure and negative pressure theories implicitly assume that the CSF is less dense than brain tissue whereas the CSF theory assumes that CSF is denser than brain tissue by about 4%.

It turns out that no one theory is able to explain all observed pathological findings in different accident scenarios. More careful studies are needed for each type of accident scenarios.

1.4.3 The contrecoup–coup phenomenon: a new understanding of the mechanism of closed head injury. [24]

In 2004 Drew and Drew developed a simple model consisting of a balloon filled with water of density $1.00 g/ml$ enclosed in a clear plastic jar containing salt water of density $1.04 g/ml$, simulating the same relative densities of the CSF and brain. The initial movement of

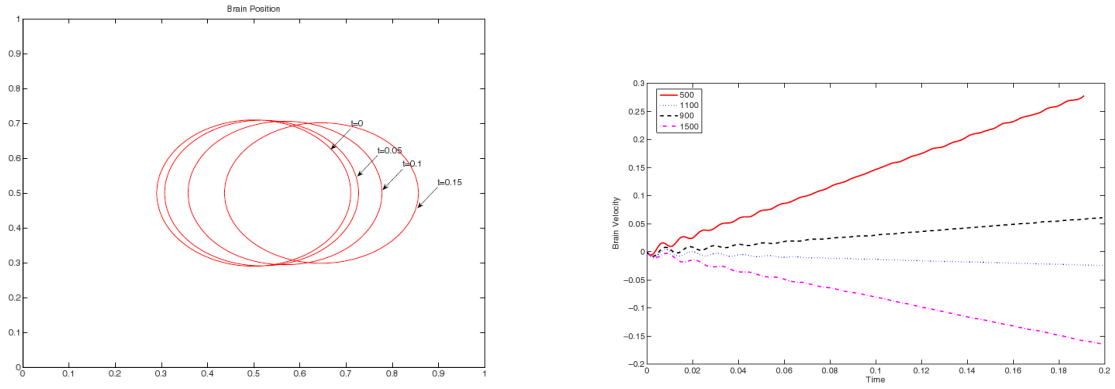

a b

Figure 1.7: Brain position at different time steps (a) and brain velocity with different brain densities (b)

the balloon, modeling the brain, was toward the contrecoup location with subsequent movement toward the coup location.

Having a diameter slightly less than the jar, the balloon did not quite contact the upper surface of the jar. Thus, the balloon was free to move horizontally in any direction as a result of the forces applied to it. The skull-CSF-brain model was propelled laterally along the horizontal table surface at approximately 1 $^{m}/_{s}$ into a hard, fixed vertical surface causing the container to abruptly stop.

Results and conclusions

Figure 1.8 shows the sequence of movements of the balloon of 1.00 $^{g}/_{ml}$ density in a jar containing salt water of 1.04 $^{g}/_{ml}$ density. A fixed marker was placed on the outside of the jar to serve as a reference point to detect movement of the balloon relative to the marker. Figure 1.8a shows the initial position of the balloon at the instant of impact. In figure 1.8b there is slight movement of the balloon away from the site of impact. Figure 1.8c shows the balloon is clearly displaced farther from the site of impact in the contrecoup direction. At this time, the displacement of balloon was at its approximate maximum displacement in the contrecoup direction. Figure 1.8d, at which time there is some subsequent secondary movement back toward the site of impact in the coup direction. The slowness of these movements was somewhat surprising and attributed to the closeness of the densities of the balloon and surrounding water.

In conclusion, in a closed head injury in which the skull is abruptly stopped, the brain has a tendency to be displaced by the denser CSF. If the extent of deceleration produces sufficient force to cause displacement of the brain relative to the skull, the initial movement of the brain will be in a direction away from the location of skull impact, resulting in initial impact of the brain with the internal surface of the skull at the contrecoup location. This initial displacement of the brain toward the contrecoup

location results in the contrecoup injury being of greater severity than the coup injury. This phenomenon provides a logical explanation for the commonly observed finding of a larger contrecoup injury as compared to the coup injury in cases of closed head injury of sufficient force so as to produce brain contusions.

a) instant of impact

b) half second after impact

c) one second after impact

d) two seconds after impact

Figure 1.8: The sequence of movements of the balloon.

1.5 Scope of the project

During this project the mechanics of the human during a closed head impact will be investigated. The impact will be applied at the front of the head. Especially the flexibility of the skull is of main interest. The influence of the flexibility/stiffness of the skull is not yet investigated in literature and it is believed it has influence during the impact. The stiffness is a very interesting parameter in child safety. Small children have thinner softer skulls and there is a debate ongoing about how this influences the brain injury risk at impact. Besides the skull stiffness, also the density of the CSF will be a variable during the simulations, because it has a great influence on the movement of the brain due to inertia.

In short, the goal is to implement these four simulations:

- Flexible skull with the density of the CSF higher than the density of the brain.
- Rigid skull with the density of the CSF higher than the density of the brain.
- Flexible skull with the density of the CSF lower than the density of the brain.
- Skull 25% less stiff than the first simulation and with the density of the CSF higher than the density of the brain.

2 Methodology

2.1 ANSYS Workbench

Ansys Workbench is a finite element method (FEM) which is a numerical technique for finding approximate solutions of partial differential equations (PDE) as well as of integral equations. The solution approach is based either on eliminating the differential equation completely (steady state problems), or rendering the PDE into an approximating system of ordinary differential equations, which are then numerically integrated using standard techniques such as Euler's method.

The finite element method shares a structure in a finite number of elements and will link these elements together through nodes. On those links, depending on the type of element, a number of requirements will be set. For example, the nodes of the elements should move together at the same time. Determination of the nodes and links correspond to the definition of a grid. The finer this mesh is, the better does the calculation approximate the real behavior, but the more calculation time is required.

A dynamic equivalent equation is required in FEM modeling for the impact analysis for this study. Ansys Workbench is using the dynamic equivalent equation at a time, t, for the FE analysis as follows:

$$[M]\{\ddot{u}(t)\} + [C]\{\dot{u}(t)\} + [K]\{u(t)\} = \{R(t)\} \tag{2.1}$$

where $[M]$ is a mass matrix, $[C]$ is a damping matrix and $[K]$ is a stiffness matrix. And $\{\ddot{u}(t)\}$, $\{\dot{u}(t)\}$, and $\{u(t)\}$ represent an acceleration vector, a velocity vector and a displacement vector at time t, respectively. The aim is the determination of the displacement vector $\{u(t)\}$ to calculate the stresses and strains and thus to determine the strength of the structure under load $\{R(t)\}$.

The finite element method is comprised of three major phases:

1. Pre-processing, here the program develops a finite element mesh to divide the subject geometry into subdomains for mathematical analysis, and applies material properties and boundary conditions. In this case the skull, CSF and brain, see section 3.1.

2. Solution, during which the program derives the governing matrix equations from the model and solves for the primary quantities.

3. Post-processing, where the program checks the validity of the solution, examines the values of primary quantities, such as displacements and stresses, and derives and examines additional quantities. These are the results of the simulation.

2.2 ANSYS CFX

Ansys CFX is computational fluid dynamics (CFD) program, which deals with the behavior of fluids, thus liquids or gases. It includes the interaction of these media and solids, combustions and reactions and also thermodynamic heat transfer. Ansys CFX, is based on the finite volume method (FVM), which is similar to the finite element method. FVM recasts the PDE's of the Navier Stokes equation in the conservative form and then discretize this equation. This guarantees the conservation of fluxes through a particular control volume. The Navier Stokes equations deal with the preservation of mass and energy and the momentum balance. These equations arise from applying Newton's second law to fluid motion, together with the assumption that the fluid stress is the sum of a diffusing viscous term plus a pressure term.

The Navier Stokes equations are strictly a statement of the conservation of momentum. In order to fully describe fluid flow more information is needed; the conservation of mass, the conservation of energy and the equation of state.

The statement of the conservation of mass is achieved through the **mass continuity equation**, given in its most general form as:

$$\frac{\partial \rho}{\partial t} + \nabla \cdot (\rho \dot{\mathbf{u}}) = 0 \tag{2.2}$$

The first term is the rate of change in time of the density. The second term describes the net flow mass out of the element across its boundaries and is called the convective term, where $\dot{\mathbf{u}}$ is the velocity vector.

The **total energy equation** has to be implemented for any compressible flow problem in Ansys CFX. It is an alternative form of the **conservative energy equation**:

$$\frac{\partial (\rho h_{tot})}{\partial t} - \frac{\partial p}{\partial t} + (\rho \dot{\mathbf{u}} h_{tot}) = \nabla \cdot (\lambda \nabla T) + \nabla \cdot (\dot{\mathbf{u}} \boldsymbol{\tau}) + \dot{\mathbf{u}} \cdot \mathrm{S_M} + \mathrm{S_E} \tag{2.3}$$

h_{tot} describes the total specific enthalpy which is related, in ANSYS CFX, to the static enthalpy $h(p, T)$ by:

$$h_{tot} = h + \frac{\dot{\mathbf{u}} \cdot \dot{\mathbf{u}}}{2} \tag{2.4}$$

The term $\nabla \cdot (\lambda \nabla T)$ denotes the divergence of the heat flux going into the control volume, $\nabla \cdot (\dot{\mathbf{u}} \boldsymbol{\tau})$ is called the viscous work term and represents the work due to the viscous stresses, $\dot{\mathbf{u}} \cdot \mathrm{S_M}$ represents the work due to an external momentum and $\mathrm{S_E}$ is a source term for the energy which is transferred over the boundaries. [25]

2.2.1 Compressible fluid

There are some phenomena that are closely linked with fluid compressibility. One of the obvious examples is sound. Description of such phenomena requires more general presentation of the Navier Stokes equation that takes into account fluid compressibility. If viscosity is assumed a constant, one additional term appears, as shown here [1]:

$$\rho\left(\frac{\partial \dot{u}}{\partial t}+\dot{\mathbf{u}}\cdot\nabla\dot{\mathbf{u}}\right)=-\nabla p+\mu\nabla^2\dot{\mathbf{u}}+\left(\frac{1}{3}\mu+\mu^v\right)\nabla\left(\nabla\cdot\dot{\mathbf{u}}\right)+\mathbf{f} \tag{2.5}$$

where μ^v is the volume viscosity coefficient, also known as second viscosity coefficient or bulk viscosity. This additional term disappears for an incompressible fluid, when the divergence of the flow equals zero. [26, 27]

To define a fluid in Ansys CFX as compressible it has to be implemented with pressure dependent density function:

$$\rho=\rho\left(p\right) \tag{2.6}$$

The relation between the change of the pressure and the change of the volume is defined as:

$$\mathrm{d}p=-\frac{1}{\kappa V}\mathrm{d}V \tag{2.7}$$

The density can be written as:

$$\rho=\frac{m}{V}\quad and\quad \frac{\partial\rho}{\partial V}=-\frac{m}{V^2} \tag{2.8}$$

$$\mathrm{dV}=-\frac{\mathrm{V}^2}{\mathrm{m}}\mathrm{d}\rho=-\frac{\mathrm{V}}{\rho}\mathrm{d}\rho \tag{2.9}$$

Inserting 2.8 and 2.9 in 2.7 gives:

$$\mathrm{d}p=\int_{p_0}^{p}1\mathrm{d}p=\int_{\rho_0}^{\rho}\frac{1}{\kappa\rho}\mathrm{d}\rho \tag{2.10}$$

$$\triangle p=(p-p_0)=\frac{1}{\kappa}\ln\left(\frac{\rho}{\rho_0}\right) \tag{2.11}$$

$$\rho\left(\triangle p\right)=\rho_0\exp^{\kappa\triangle p} \tag{2.12}$$

The term p denotes in this equation the absolute pressure, where one density value ρ_0 must be known for the corresponding pressure. The pressure p_0 is not assigned so it can be set equal to the reference pressure $p_0=p_{ref}$ where $\rho_0=\rho_{ref}=\rho\left(p_{ref}\right)$, which characterizes the density for the reference pressure. So $\triangle p$ equals the static pressure, as $\triangle p=p-p_{ref}=p_{stat}$. κ is the isothermal compressibility term, which is the inverse of the Bulk modulus. Note that despite this fact the static pressure can not be used in the density function in Ansys CFX. It still has to be written as the difference of the absolute pressure and the reference pressure, since Ansys CFX substitutes instantly the static pressure in a function with the absolute pressure:

$$p_{stat}=p_{abs}-p_{ref} \tag{2.13}$$

So the expression, as function of the pressure, which will be used in Ansys CFX-Pre to describe the compressible CSF is:

$$\rho\left(\triangle p\right) = \rho_0 \exp^{\kappa\left(p_{abs} - p_{ref}\right)} \tag{2.14}$$

Bulk modulus

The properties of CSF are very water-like. If it is assumed, that the speed of sound in CSF and water is comparable, the Bulk modulus β can simply be denoted by transforming the following equation:

$$c = \sqrt{\frac{\beta}{\rho}} \quad \Longrightarrow \quad \beta = \rho c^2 \tag{2.15}$$

The isothermal compressibility term κ is the inverse of the Bulk modulus, this leads to:

$$\kappa = \frac{1}{\beta} = \frac{1}{\rho c^2} \tag{2.16}$$

where c is the speed of sound in the medium and ρ is the density of the fluid. Now it is possible to determine the isothermal compressibility term of the CSF and the brain, see table 2.1.

Material	ρ $(at\ 37°C)$	c	κ
Water	$991.27\ ^{kg}/_{m^3}$	$1520\ ^{m}/_{s}$	$4.37 \cdot 10^{-10}\ Pa^{-1}$
CSF[1]	$1006\ ^{kg}/_{m^3}$	$1492\ ^{m}/_{s}$	$4.47 \cdot 10^{-10}\ Pa^{-1}$
Brain	$1024\ ^{kg}/_{m^3}$	$1530\ ^{m}/_{s}$	$4.17 \cdot 10^{-10}\ Pa^{-1}$

Table 2.1: Isothermal compressibility

2.3 Coupling method [25]

The simulation of this study requires coupling between the CFX solver and ANSYS structural solver, because the solids, skull and brain, are modeled in ANSYS WORKBENCH and the CSF (fluid) is modeled in ANSYS CFX. The coupled simulation follows a time step/iteration structure.

In ANSYS multi-field solver, data are communicated between the ANSYS CFX and ANSYS Structural field solvers through standard Internet sockets using a custom client-server communication protocol. Setup requires creation of the fluid and solid domain/physical models in the ANSYS CFX and ANSYS WORKBENCH user interfaces, respectively, and the specification of coupling data transfers and controls in the ANSYS CFX user interface. Execution and run-time monitoring of the coupled simulation are performed from the ANSYS CFX solver manager.

[1] Because the density of the CSF is a variable during the simulatons also κ will change.

An Ansys input file, which contains the Ansys setup for the structural problem, including the identification of the Fluid Solid Interfaces on the Ansys Workbench (solids) model, must be written. This will be attached to the Ansys CFX simulation to determine the valid interfaces for selection later on, and will also be used by default as the ansys input file when the solver run is started from Ansys CFX solver manager. Coupled simulations begin with the execution of the Ansys structural- and CFX field solvers. The Ansys structural solver acts as a coupling master process to which the CFX solver connects. During every staggerededed iteration, each field solver gathers the data it requires from the other solver, and solves its field equations for the current coupling step. staggereded iterations are repeated until a maximum number of staggereded iterations is reached or until the data transferred between solvers and all field equations have converged. The latter guarantees an implicit solution of all fields for each coupling step.

3 The model

3.1 Pre-processing

Geometry and meshing

In order to create the model, first of all the geometry has to be built. For that task the Ansys Workbench *design modeler* is used and the geometry would consist in three parts, two solids and one liquid. The solid parts are the brain, the skull, and they are built independently of the liquid part, because the manner that a CFD solve its problems is different than the FEM does, despite of its similar procedure.

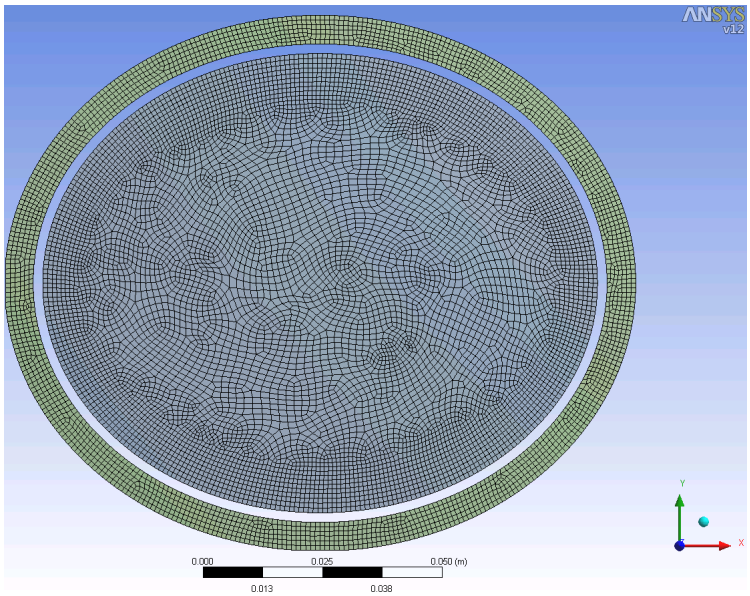

Figure 3.1: Mesh of the skull and the brain

In order to achieve a proper mesh the body has been separated in three different parts, the skull, CSF and the brain. For the mesh of the three parts two different meshing controls have been used. These are *edge- face sizing control*. With this meshing control tools it is possible to choose the element size. This is important because the geometry is 3D, but a fluid solid interaction (FSI) in Ansys requires a 2D model. In order to make the geometry 2D, the number of elements in the z-direction should be one, see figure 3.2. With the use of *face sizing control* it is possible to select the faces which should have a thickness of one element. This option has also a really big influence on the calculation

time. *edge sizing control* gives the opportunity to set the size of the element. As shown in figure 3.1, the size of the elements close to edge of the brain are smaller than the element close to the middle. This is because of accuracy of the interaction with the fluid during the simulation. The elements of the CSF and the elements at the borders of the skull and brain have the same size, this for the same reason.

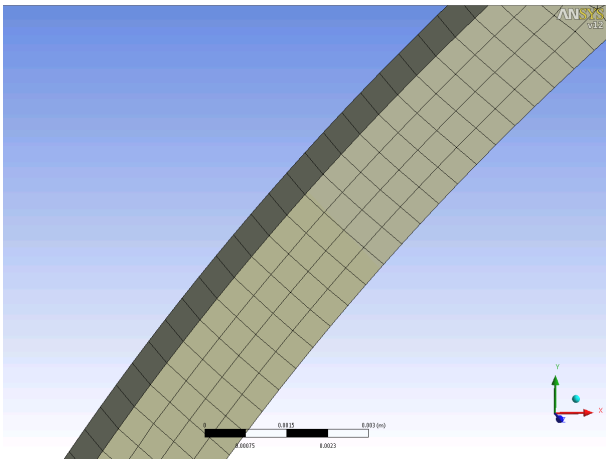

Figure 3.2: Mesh of the CSF with one element in the z-direction

FEM configuration

When the geometry and the mesh of the parts are created, it is time to set the FEM configuration. Because the simulation is a time dependent deformation the option *flexible dynamic* should be chosen. The time step $\triangle t = 3 \cdot 10^{-5}\ s$ and the end time is $t_{end} = 3 \cdot 10^{-3}\ s$. The time step and end time are a personal choice. They can be changed before every simulation. The end time of $3 \cdot 10^{-3}\ s$ is chosen this small because otherwise the calculation is taken to much time. The time of $3 \cdot 10^{-5}\ s$ is enough to study the effect of the wave propagation.

Like mentioned for the communication with the fluid part at the boundary walls *fluid solid interfaces* have to be implemented, these are the outside wall of the brain and the inside wall of the skull. For no movement in z-direction *frictionless supports* at the xy walls of the bodies are created. Also the load at the forehead is generated as time dependent accelerating deformation in the x-direction. Finally an Ansys input file is written, which includes the whole setup and will be attached to the CFX simulation.

Material properties

As mentioned in section 1.2.3 Francheschini [19] did an interesting research to material properties of the human brain. He used the Ogden's model to describe these properties. In Ansys it is possible to use this model for a material. Ansys uses the following equation:

$$\mathbf{\Psi_{def}}(J) = \sum_{i=1}^{M} \frac{1}{d_i} (J-1)^{2i} \tag{3.1}$$

For $M = 1$, $d_1 = \frac{2}{\beta}$, where β is the bulk modulus, see section 2.2.1.

Material	ρ $[kg/m^3]$	α $[1/°C]$	E $[Pa]$	ν	μ $[Pa]$	A_1	d_1 $[1/Pa]$
Skull	1420	0.1	$6.5 \cdot 10^9$	0.22			
Brain	1042	0.1			290.82	6.19	$8.34 \cdot 10^{-10}$

Table 3.1: Material properties of the solid parts

α is the coefficient of thermal expansion, E is the Young's modulus and ν is the Poisson ratio. μ, A_1 and d_1 are Ogden parameters.

CFD configuration

The Ansys CFX simulation type is *transient* and the *coupled solver* is enabled. The fluid is setup to be compressible, which requires the *total energy equation* as *heat transfer* option. In this scenario the compression is mainly pressure dependent, so nearly no heat transfer is expected, but it is not possible to avoid this heat exchange equation in Ansys CFX in this case. The speed of the CSF is expected to be very low, so a *laminar flow* was selected. The *under relaxation factor* can be set to 0.9, the basic value is 0.7, because of the stability which is generated by the substitution of the load. Disadvantage of the relaxation factor is that the calculation time will be a lot longer. When the CFX solver will run, the solver of the Workbench will be started automatically.

CSF material properties

The CSF has been modeled with the properties of water, because its properties are very water-like; the value for the density will be changed for the different simulations. When the density of the CSF is higher than the brain it is 1100 kg/m^3 and if it is lower it will be 1080 kg/m^3. Thus in Ansys CFX water will be chosen as material, but the density will be an expression, see section 2.2.1, which is as function of the pressure. ρ_0 will be the starting density of the CSF.

3.2 Solution

During the calculation the solver generates a curve plot, for the visual *convergence control*, on the screen. For a common transient simulation the summarized residuals of any field equations are printed at any iteration step. At the coupled simulation the residual output is a bit uncommon. During every iteration-step a value e, which is an indicator for the change of the calculated loads and deformations in every boundary point. First the term Ψ is calculated, which represents the totalized, normalized change of the loads

and deformations in the interfaces, see equation 3.2. This term is logarithmized, subtracted by the logarithm of Ψ_{min}, the convergence target, which has to be defined by the observer before, and scaled by the difference of 2 and the logarithm of Ψ_{min} , see equation 3.3. This is generally positive as the *convergence target* is much smaller than 1. The reason for this uncommon output is the following: The deformations of the boundary walls result from forces which are unknown. So the balance point of deformation and forces is not known. The only opportunity to make a convergence visible is to plot a transformed indicator of the changes in the interfaces. If these become smaller it can be expected that the solution gets closer to a balanced state in the interface regions. If the changes are smaller than the *convergence target* the curve becomes negative, which can be, depending on the size of the *convergence target*, an indicator for convergence.

$$\Psi = \sqrt{\left(\frac{u_{new} - u_{old}}{u_{new}}\right)^2} \tag{3.2}$$

$$e = \frac{\log\left(\frac{\Psi}{\Psi_{min}}\right)}{\log\left(\frac{100}{\Psi_{min}}\right)} \tag{3.3}$$

where u_{new} is the load transferred this staggereded iteration step and u_{old} denotes the load transferred in the last staggereded iteration step. The solid part transfers the wall deformation information to the fluid dynamics part, which gives back the forces on the wall. So the WORKBENCH solver simply calculates the deformation of the wall caused by some kind of load, defined as a boundary condition. This is a common solid mechanics problem, so there is a simple residual output of the force and the deformation. The residuals for the transient simulation are plotted for every time step [1, 25].

4 Results

During this project, until shortly before the end, very interesting results were received by the program. Unfortunately there was a calculation error discovered in the earlier work of this study. It concerns the value of the isothermal compressibility. The correct value of this parameter gave many problems during the subsequent simulations. Especially the mesh-movement of the brain was a major problem. This could be solved by a very fine mesh, but it caused a very long computation time (the first three time steps from one hundred took about 24 hours). The previous results are not 100% trusting and that is why in this chapter the results of Sans and Aracil [2] will be discussed.

4.1 The model

The model of Sans and Aracil is almost the same as the model used for this study, see figure 4.1. Also the material properties of the solids and the CSF are nearly equivalent. In their project they ran two different simulations. In the second simulation they multiplied the value of the Young's modulus of the skull and neck with a factor of 1000, because they wanted to run a simulation with a rigid skull. This is the first point which could be improved, because a multiplication of the Young's modulus does not make the material 100% rigid. It is possible to select the complete skull and neck and displace it with the time dependent accelerative deformation in the x-direction.

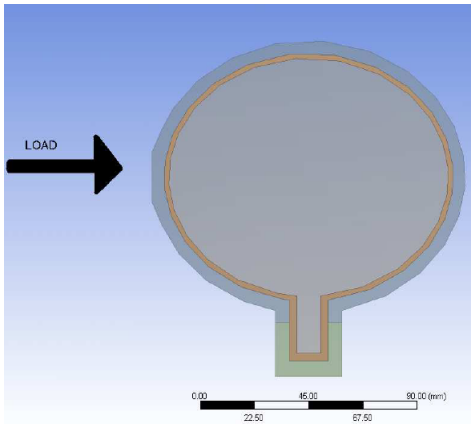

Figure 4.1: ANSYS model Sans and Aracil [2]

4.2 Results

In figure 4.2 the elastic equivalent strains in the brain are shown of the first simulation. It looks like there is something happening at the contrecoup site of the brain during the frontal impact. Clearly their is a lot of strain at that site of the brain. Also these simulations have used the wrong isothermal compressibility term.

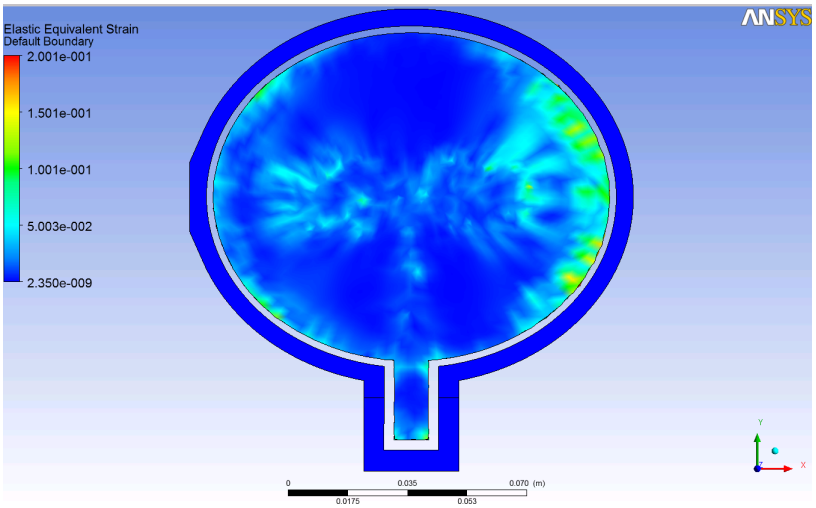

Figure 4.2: Simulation 1: Elastic equivalent strain in the brain

However, if we look closer at the results (figure 4.3) it is clear to see that the strains are caused by the mesh movement and not by the frontal impact. This mesh behavior can be avoided by taking a smaller element size. When a simulation with a smaller element size in the mesh was executed the strains were no longer there.

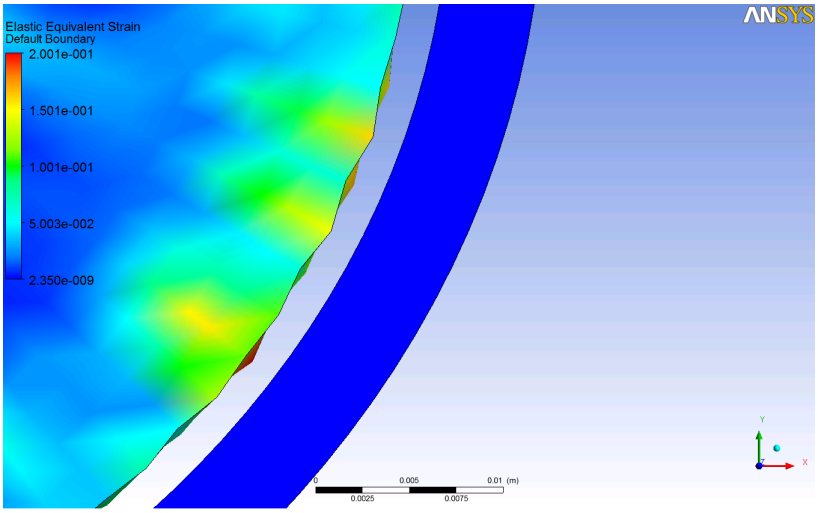

Figure 4.3: Simulation 1: Elastic equivalent strain in the brain (zoomed in)

Also in the second simulation the same problem is visible. Despite the stiffness of the skull is multiplied by a factor 1000, still there are some strain in the brain, especially at the location of the neck. This is shown is figure 4.4.

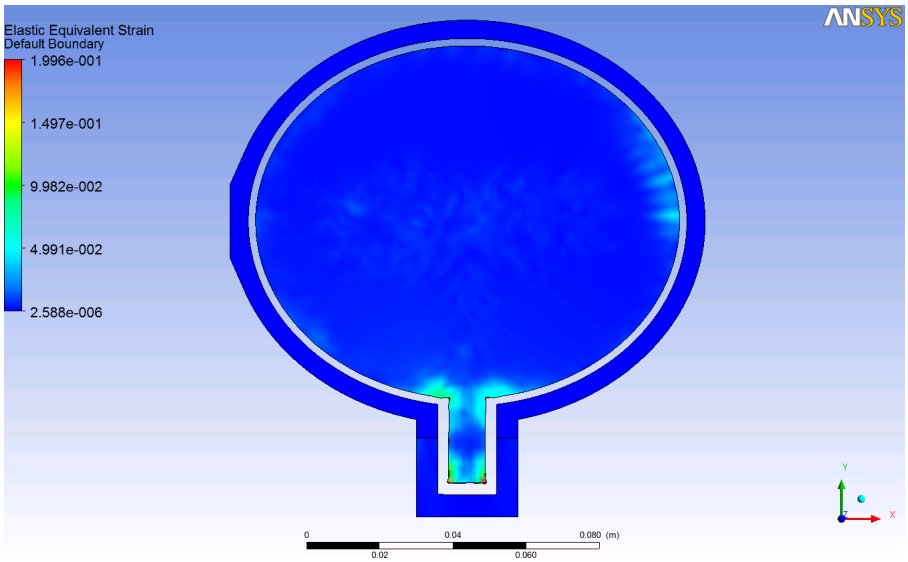

Figure 4.4: Simulation 2: Elastic equivalent strain in the brain

Again if we look closer at the result the same problem is happening. This time, the wrong mesh displacement is even shown better than in the results of the first simulation.

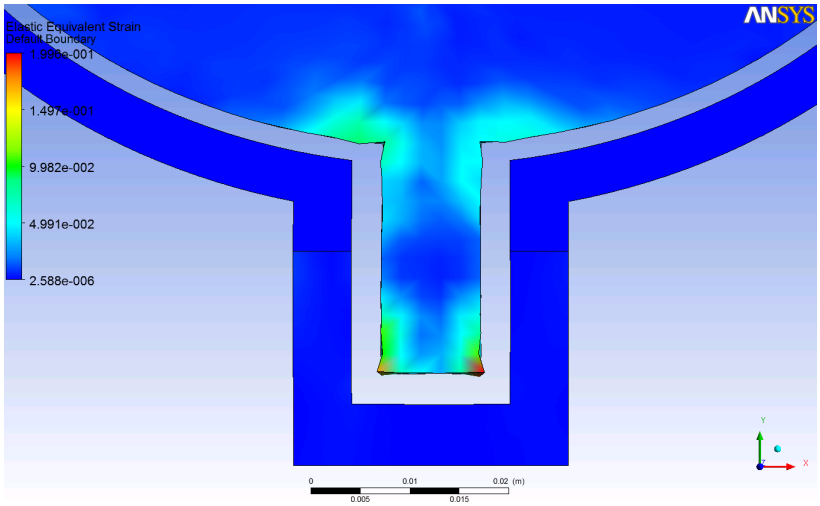

Figure 4.5: Simulation 2: Elastic equivalent strain in the brain (zoomed in)

5 Conclusion and recommendations

The aim of this project was to create a FEM model which would give new insights on brain injuries. In particular the influence of the flexibility of the skull during a frontal impact against the forehead was of great interest. During the project it showed that the modeling of human head is very difficult to achieve. Although the model, in terms of geometry, was very simple, a good working impact simulation was very difficult to achieve. One of the main reasons for this problem was the wrong value of the isothermal compressibility which is causing really strange mesh behavior. Also the material properties of the brain are likely to affect the strange motion of the mesh during the simulations. One of the recommendations is to use a different model to describe the brain, instead of the current use Ogden's model. For example, a linear elastic material model. Another recommendation is to give much attention to the modeling of the mesh. During the project it was shown that the modeling of the mesh had significant impact on the results.

Another subject of interest is the velocity of the fluid of the CSF. It is assumed that the flow should be very low, but during the simulations the speed reaches sometimes a higher value than the border of turbulence, which is around $0.8\ ^{m}/_{s}$. For future work, this fluid velocity should be of big interest.

The last recommendation is to keep an eye on the value of the time step. Sometimes a smaller time step is giving better mesh behavior and also calculation time is improving, which is normally the opposite.

Despite the fact that there were a lot of problems at the end of the project, it is believed that the flexibility of the skull has an influence on the brain injuries during a closed head impact. Still there is a lot work to do in this research to improve vehicle safety and to improve the understanding of brain injuries during a closed head impact.

Bibliography

[1] Fliedner J. (2008) ”Development of a Brain Model for Simulations of Diverse Types of Injuries”. Department of Applied Mechanics. Chalmers University of Technology. Göteborg Sweden

[2] Sans J.M., Aracil J.C. (2009) ”Numerical simulation in traffic-related brain injuries”. Department of Applied Mechanics. Chalmers University of Technology. Göteborg Sweden

[3] Maas A.I., Stocchetti N., Bullock R. (August 2008). "Moderate and severe traumatic brain injury in adults". Lancet Neurology 7 (8): 728–41.

[4] León-Carrión J., Domínguez-Morales Mdel R., Barroso y Martín J.M., Murillo-Cabezas F. (2005). "Epidemiology of traumatic brain injury and subarachnoid hemorrhage". Pituitary 8 (3-4): 197–202.

[5] Park E., Bell J.D., Baker A.J. (April 2008). "Traumatic brain injury: Can the consequences be stopped?". Canadian Medical Association Journal 178 (9): 1163–70.

[6] Langlois J.A., Rutland-Brown W., Wald M.M. (2006). "The epidemiology and impact of traumatic brain injury: A brief overview". Journal of Head Trauma Rehabilitation 21 (5): 375–8.

[7] http://www.hopkinsmedicine.org/craniofacial/LynmProject/BSC/BSC1.HTM

[8] Lynnerup N.,Astrup J.G., Sejrsen B. (December 2005). ”Thickness of the human cranial diploe in relation to age, sex and general body build”. Head&Face Medicine, 1:13

[9] Peterson J., Dechow J.C. (2002). ”Material Properties of the inner and outer cortical tables of the human parietal bone”. The anatomical record. 268:7-15

[10] Delill R., Lesueur D., Potier P., Drazetic P., Markiewicz E. (2007) ”Experimental study of the bone behaviour of the human skull bone for the development of a physical head model”. International Journal of Crashworthiness, 12:2, 101-108

[11] Marieb E.M., (1998) ”Human Anatomy and Physiology”. Fourth edition. Addison-Wesley

[12] Saunders N.R., Habgood M.D., Dziegielewska K.M. (1999). "Barrier mechanisms in the brain, I. Adult brain". Clin. Exp. Pharmacol. Physiol. 26 (1): 11–9.

[13] Felgenhauer K. (1974). "Protein size and CSF composition". Klin. Wochenschr. 52 (24): 1158–64

[14] Richardson M., Wissler R. (1996). "Density of Lumbar Cerebrospinal Fluid in Pregnant and Nonpregnant Humans". Anesthesiology. 85(2):326-330

[15] Levin E., Muravchick S., Gold M.I. (1981). "Density of Normal Human Cerebrospinal Fluid and Tetracaine Solutions". Anesth Analg 1981; 60:814-817

[16] http://biology.about.com/od/humananatomybiology/a/anatomybrain.htm

[17] Cosgrove K.P., Mazure C.M., Staley J.K. (2007). "Evolving knowledge of sex differences in brain structure, function, and chemistry." Biol Psychiat 62: 847–55

[18] Lynn R. (Aug 1994). "Sex differences in intelligence and brain size: A paradox resolved." Personality and Individual Differences Vol 17 (2): 257-271

[19] Parent A. Carpenter M.B. (1995). "Carpenter's Human Neuroanatomy". Williams & Wilkins. Ch 1.

[20] Franceschini G. (2006). "The mechanics of human brain tissue". Ph.D. Thesis, University of Trento

[21] Moritz A.R. (1943). "Mechanisms of head injury". Ann Surg.; 117(4): 562–575.

[22] Anderson T., Heitger M., Macleod A.D. (2006). "Concussion and mild head injury". Practical Neurology 6: 342–57.

[23] Mishra A., Mohanty S. (2001). "Contre-coup extradural haematoma : A short report". Neurology India 49 (94): 94.

[24] Smith D.H., Meaney D.F. (2000). "Axonal damage in traumatic brain injury". The Neuroscientist. 6 (6): 483—495.

[25] Belingardi G., Chiandussi G., Gaviglio I. (2005). "Development and validation of a new finite element model of human head". Technical report, Politecnio di Torino, Dipar- timento di Meccanica

[26] Halabieh O., Wan J.W.L. (2008). "Simulating Mechanism of Brain Injury During Closed Head Impact". F. Bello, E. Edwards (Eds.): LNCS 5104, pp. 107–118

[27] Drew L.B., Drew W.E. (2004). "The contrecoup-coup phenomenon: a new understanding of the mechanism of closed head injury". Neurocritical Care 2004;1:385–90

[28] ANSYS release 11.0 Engineering Data Help, 2007

[29] Landau & Lifshitz (1987) pp. 44–45.

[30] Batchelor (1967) pp. 147 & 154.